



## Simultaneous activation of *Ficus carica* L. leaves for the removal of emerging pollutants from aqueous solutions

Zohra Mekibes, Benaouda Bestani\*, Nadia Douara, Noureddine Benderdouche, Mokhtar Benzekri-Benallou

Laboratoire Structure, Elaboration et Application des Matériaux Moléculaires, Université Abdelhamid Ibn Badis de Mostaganem, Algeria, Tel. +213552329407; email: bestanib@yahoo.fr (B. Bestani), Tel. +213 792623929; email: zorahamadi@yahoo.fr (Z. Mekibes), Tel. +213 674305658; email: nadia.douara@yahoo.fr (N. Douara), Tel. +213 772618906; email: benderdouchen@yahoo.fr (N. Benderdouche), Tel. +213 674305637; email: benzekrimokhtar@yahoo.fr (M. Benzekri-Benallou)

Received 5 August 2020; Accepted 25 January 2021

### ABSTRACT

*Ficus carica* L. leaves, endemic in the Mediterranean region, are chosen as a lignocellulosic source of raw material for the preparation of activated carbon by simultaneous activation by impregnating the raw material in 85%  $H_3PO_4$  for 3 h at 100°C and then pyrolyzing the slurry at 600°C. The prepared activated carbon was used for the removal of two emerging pollutants paracetamol and amoxicillin.  $N_2/77$  K adsorption experiments on the prepared activated carbon resulted in a Brunauer–Emmett–Teller specific surface area of 658  $m^2/g$ . Fourier-transform infrared analysis, Boehm titration, and  $pH_{zpc}$  determination were performed to characterize surface functional groups and the acidic nature of the prepared material. The effect of several parameters including adsorbent dose, solution pH was evaluated. Adsorption isotherms were better described by the Langmuir model than those of Freundlich and Temkin. The maximum adsorption capacities achieved for paracetamol and amoxicillin were 53.28 and 44.67 mg/g, respectively. Kinetics was found to obey the pseudo-second-order model. This study shows that activated *Ficus carica* L. can be successfully used as a new adsorbent for the treatment of water laden with such as contaminants.

**Keywords:** Activated carbon; Characterization; *Ficus carica* L; Emerging pollutants; Adsorption

### 1. Introduction

Water is a vital element among the natural resources, crucial for the survival of all living organisms, and essential to our health. Many industries use water extensively in their production process and discharge thereby large quantities of organic and inorganic pollutants into the environment without often any prior treatment with a negative impact on human lives and public health. Recent studies have shown the presence of a wide variety of emerging pollutants in wastewater, generally without regulatory environmental status [1,2], as for instance,

certain medicinal substances for human or veterinary uses including detergents, disinfectants, etc. [2–4].

Most of these identified substances are suspected of having effects on endocrine functions and of causing problems to human health and the ecosystem [4,5].

Pharmaceuticals are increasingly entering wastewater through disposal and excretion. They have been detected in effluents and aquatic environments as early as the 1980 s, but recently, studies revealed the presence of more than 80 pharmaceuticals in wastewater effluents [6]. Measures are being taken to limit their potential impact on wastewater. This has led to increased interest in the research

\* Corresponding author.

and development of these products and their environmental and health impacts [7]. Pharmaceuticals present in wastewater at high concentrations include antibiotics and a wide range of analgesics, antiseptics, anti-inflammatory drugs, and antidepressants.

The two adsorbates chosen in this study, paracetamol and amoxicillin, are emerging pollutants because they are widely spread in the aquatic environment. Their presence in the environment in concentrations that do not comply with pollution legislation is unacceptable and their elimination from waste effluents is becoming an imperative need and an environmental importance.

Many techniques have been used to remove pharmaceuticals from wastewater, such as biological processes [8], advanced oxidation processes [9], and electrocoagulation [10,11].

All of these methods have inherent advantages and limitations. Adsorption technology has become a very efficient and simple method to use.

Adsorption is widely used to effectively trap all kinds of pollutants from wastewater [12–14] using solids as adsorbents such as clay, zeolite, activated alumina, and activated carbons. The latter, with a high surface area, pore structure, and a high degree of surface reactivity, are very useful adsorbents. They are also economical adsorbents for many industrial applications.

As commercial activated carbons are relatively expensive, various studies have been carried out on the development of efficient adsorbents from a wide variety of base materials such as coconut shells [15,16], olive pits [17,18], date pits, sawdust, and other fruit pits [19–21].

It is with this in mind that this work is carried out to valorize *Ficus carica* L. leaves into activated carbon. Simultaneous chemical and thermal activations were applied. Several chemical agents, such as phosphoric acid, zinc chloride,

sodium hydroxide, potassium among others, are widely used as oxidizing agents for chemical activation [22,23]. The resulting activated carbons are cheaper than commercial carbons, and are effective as adsorbents to remove a variety of toxic pollutants.

Our choice was based on the elimination of two commonly used drugs and emerging pollutants, paracetamol and amoxicillin. Paracetamol, an analgesic and antipyretic, is prescribed for the treatment of moderate symptoms [24,25]. Amoxicillin, a  $\beta$ -lactamine penicillin antibiotic, acts against multiple bacterial infections because of its broad spectrum of antimicrobial activity and low toxicity [26].

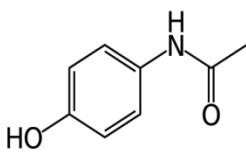
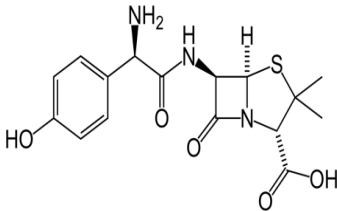
## 2. Material and methods

### 2.1. Adsorbent and adsorbate preparation

Stock solutions of the relevant substances of paracetamol and amoxicillin (Saidal – Algeria, 99% purity) of known concentrations were prepared according to the standard procedure by dissolving 500 mg of each substance in 1 L flasks. Distilled water was added up to the 1 L mark. Stock solutions were diluted were used to prepare working solutions of lower concentrations. Table 1 shows some properties of paracetamol and amoxicillin.

*F. carica* L. fig is an abundant lignocellulosic plant endemic to the Mediterranean region. Fig leaves were collected in the Mostaganem region of western Algeria and used as a precursor for the preparation of activated carbon. The raw material was washed to remove dust, dried at room temperature for several days, crushed using a CrosschopVierzen grinder, and finally sieved to a size of 0.14 mm. The resulting sample was again washed several times until the color was completely faded and then dried overnight in the 105°C oven.

Table 1  
Chemical structure and characteristics of emerging pollutants

	Paracetamol	Amoxicillin
Molecular structure		
Chemical formula	C <sub>8</sub> H <sub>9</sub> NO <sub>2</sub>	C <sub>16</sub> H <sub>19</sub> N <sub>3</sub> O <sub>5</sub> S
Synonyme	N-(4-hydroxyphénol) acétamide	Acide 7-, amino-3,3-diméthyl-6-oxo-2-thia-5-azabicyclo, heptane-4-carboxylique
Molecular weight (g/mol)	151.2	365.4
Maximum wavelength $\lambda_{\max}$ (nm)	242	227
Solubility (g/L at 28°C)	14.00	3.430
*CAS number	103-90-2	26787-78-0
Chemical safety	Irritant	Irritant

\*Source: Sigma-Aldrich Chemie GmbH, Eschenstr. 5, 82024 Taufkirchen, Germany (product information)

Impregnation was carried out by mixing 40 g of the grinded *F. carica* L. leaves in 85% phosphoric acid (dehydrating agent) in the 1:1 ratio. The mixture was heated at 170°C for 2 h followed by pyrolysis at 600°C for 2 h in a NABERTHERM tubular furnace. The resulting sample was washed with HCl (0.1 M) and then rinsed several times with distilled water in a Soxhlet until neutral pH, oven-dried at 105°C for 24 h, ground with a RETSCH mill, and sieved to a diameter <0.071 mm. This size reduction is simply intended to increase its surface area and reactivity.

## 2.2. Adsorbent characterization

The resulting powdered activated carbon was first characterized before application for the removal of the pain killer and antibiotic chosen.

### 2.2.1. Physical characterization

#### 2.2.1.1. Nitrogen adsorption–desorption

$N_2/77$  K adsorption tests were carried out on the degassed resulting samples using Brunauer–Emmett–Teller (BET) surface area analyzer (Quadrachrome SI-KR/MP-Quantachrome Instruments, Boynton Beach, FL, USA) for apparent surface area determination ( $S_{BET}$ ), discrete Fourier transform analysis. Iodine number (IN) and methylene blue index (MBI) were used for micro and mesoporosity estimations, respectively.

#### 2.2.1.2. Iodine number and Methylene blue-available surface areas

Additional information about the structure of activated carbons can be obtained by various test methods which are used to characterize their ability for adsorbing molecules of different types and sizes. These include among others, the determination of the molasses number (or efficiency), IN, MBI, and  $CCl_4$  activity. The most fundamental and commonly used parameters to characterize activated carbons performance are iodine number and MBI.

As a standard measure for liquid-phase applications, the iodine number (IN) is defined as the number of milligrams of iodine adsorbed per gram of activated carbon and measures the activity level of activated carbon. The degree of activation is directly related to this number by predicting its micropore content (0–20 Å). The ASTM D4607 standard method [27] was applied for the determination of iodine number. The MBI is defined as the amount of methylene blue adsorbed on activated carbon under defined conditions. It is a qualitative indication of the mesopore structure of activated carbon and is a good indicator for the adsorption of larger molecules according to the Chemviron-Carbon Company (Zoning Industriel C. B-7181 Feluy, Belgium) TM-1 standard method. The surface area available to methylene blue is calculated by Eq. (1) [28,29]:

$$S_{BM} = \frac{b \times N_A \times A_{BM}}{M_{BM}} \quad (1)$$

where  $S_{MB}$  is the surface area ( $m^2/g$ ),  $b$  is maximum adsorption capacity ( $mg/g$ ) based on a monolayer coverage (determined

beforehand from the Langmuir model),  $N_A$  is Avogadro's number ( $6.023 \times 10^{23} \text{ mol}^{-1}$ ),  $A_{MB}$  is the surface occupied by a molecule of methylene blue (taken as  $119 \text{ \AA}^2$ ), and  $M_{MB}$  is the molecular weight of methylene blue ( $319.86 \text{ g mol}^{-1}$ ).

### 2.2.1.3. Scanning electron microscopy and X-ray photoelectron spectroscopy measurements

Micrographs images of the collected leaves were obtained with a JEOL JSM 7600 F field emission gun scanning electron microscopy (FEG-SEM) before and after activation. X-ray photoelectron spectroscopy (XPS) measurements were carried out using a Kratos Axis Ultra working with  $AlK\alpha$  (1,486.6 eV) radiation to provide information about the nature of oxygen-containing functional groups present on the activated carbon surface. High-resolution spectra were obtained at a 20 eV pass energy and an analyzer resolution energy of 0.9 eV. The C1s line of 284.5 eV (reference) was used to correct the binding energies for the charge energy shift.

## 2.2.2. Chemical characterization

### 2.2.2.1. Oxygenated functional groups determination

Boehm titration was used to determine oxygenated functional groups [30] present on the adsorbent surface by simple acid-base titration. Acids with different  $pK_a$  values are used and neutralized by bases with different strengths. Fourier transforms infrared (FTIR) analysis was also used to further evaluate the functional groups on the adsorbent surface. The classical KBr pellets method was applied using an IR Prestige-21, SHIMADZU spectrometer (Tokyo, Japan). The XPS technique was also used to analyze the surface chemistry.

### 2.2.2.2. pH of zero point of charge ( $pH_{ZPC}$ ) determination

The pH value at which the surface of an adsorbent is globally neutral (no release of either  $H^+$  or  $OH^-$  ions) is called the point of zero charge ( $pH_{ZPC}$ ). Below this point ( $pH < pH_{ZPC}$ ), the surface is positively charged (anions can be favorably adsorbed); beyond this value ( $pH > pH_{ZPC}$ ), it is negatively charged (cations can be favorably adsorbed). 50 mL of 0.01 M NaCl solutions were put into several closed Erlenmeyer flasks. Their pH values were adjusted between 2 and 12 by adding HCl (0.1 M) or NaOH (0.1 M) solutions, measured at equilibrium, and noted as  $pH_{initial}$ . An amount of 0.15 g of activated carbon was then added into each flask containing the equilibrated NaCl solutions, which were stirred magnetically for 48 h. pH was measured again and noted as  $pH_{final}$ . The  $pH_{ZPC}$  is the value at which  $pH_{initial} = pH_{final}$  as reported in previous work [31].

### 2.2.2.3. Burn-off

Burn-off is defined as the loss of mass of the material based on the initial mass used in the activation step. In this case, the burn-off of *F. carica* L. leaves can be expressed as:

$$\text{Burn-off}(\%) = \frac{\text{mass}_i - \text{mass}_f}{\text{mass}_i} \times 100 \quad (2)$$

where  $mass_i$  is the initial mass of the leaves used during activation and  $mass_f$  is the final activated carbon mass.

The samples efficiency was estimated from the following equation:

$$R(\%) = \frac{\text{Activated carbon mass}}{\text{Initial leaves mass}} \times 100 \quad (3)$$

### 2.3. Batch adsorption studies

Batch adsorption studies were carried out on the activated carbon prepared by mixing 0.1 g (4 g/L) of adsorbent with 25 mL of the chosen pollutants solutions of known concentration. The mixture was then stirred magnetically at room temperature at a constant speed. The solutions were centrifuged at 6,000 rpm for 15 min (using a Hettich EBA 8 centrifuge) after the equilibrium contact time elapsed. The supernatants were analyzed using a UV-vis (Shimadzu UV mini 1240 UV-vis Spectrophotometer, UV Shimadzu Co., Ltd., Tokyo, Japan) at 242 nm for paracetamol and 227 nm for amoxicillin. The effect of pH (2–12), initial concentration (20 and 50 mg/L), contact time (0–180 min), adsorbent dose (1–8 g/L), and temperature (25°C–45°C) was also studied in duplicate and the average values reported for further calculations. The amount of the pollutant adsorbed by the solid phase ( $q_e$ ) was determined according to the following mass balance equation:

$$q_e = \frac{V}{m} (C_0 - C_{eq}) \quad (4)$$

where  $C_0$  and  $C_{eq}$  are the initial and the equilibrium pollutant concentrations (mg/L) respectively,  $V$  the volume of the solution (mL), and  $m$  the mass of the adsorbent sample (mg).

## 3. Results and discussions

### 3.1. Material characterization

The working conditions: (impregnation mass ratio with  $H_3PO_4$  (1:1), impregnation time of 90 min at 110°C followed by heating at 600°C for 2 h) yielded a mixed microporous and mesoporous sample as shown by the obtained iodine number and MBI values of 615.68 and 142.79 mg/g, respectively (Table 2). In addition, the yield value which is close to 50% bodes good adsorptive properties.

Fig. 1 shows the pore-size distribution of (FF) and C-FF samples determined using  $N_2$  adsorption.

Fig. 2 shows the adsorption–desorption isotherms of  $N_2$  liquid (77 K) of the as-received (FF) and the activated carbon (C-FF) samples. Hysteresis, shown by both isotherms, is a clear characteristic of IV-Type isotherms according to IUPAC classification. The presence of micropores is indicated by the volume adsorbed at a low relative pressure ( $P/P_0 < 0.01$ ). From Fig. 2, one can see that the C-FF material has considerable microporosity whereas the untreated leaves (FF) show almost no microporosity, in agreement with the iodine number values determined. On the other hand, the volume adsorbed at a high relative pressure ( $P/P_0$  near 1.0) shows that C-FF has larger porosity than FF.

Table 2 shows that there is a significant effect of heating on the specific surface area. A significant increase in the

Table 2  
Physical properties of FF and C-FF, and their textural characteristics

Properties	Adsorbents	
	FF	C-FF
Yield (%)	/	49.6
Burn-off (%)	/	50.4
Iodine number (mg/g)	161.42	615.68
Methylene blue index	48.95	142.79
BET specific surface area ( $m^2/g$ )	2.99	658.4
Micropore area ( $m^2/g$ )	1.93	564.3
Mean pore diameter $d_p$ (Å)	27.69	11.78
Total pore volume ( $cm^3/g$ )	0.003	0.342
$pH_{zpc}$	/	2.95

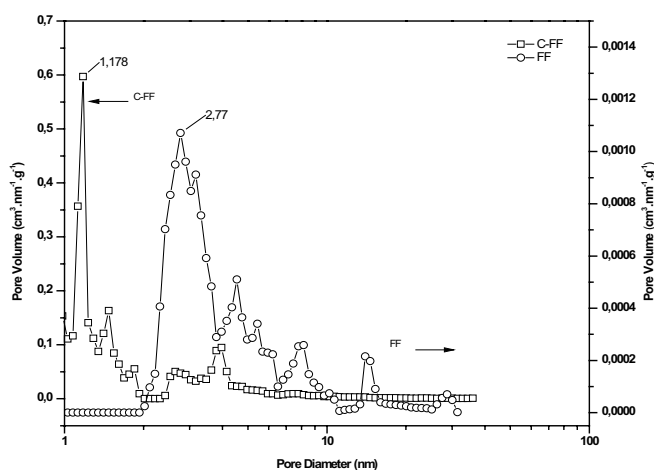


Fig. 1. Pore size distribution (PSD) of FF and C-FF from DFT,  $N_2$  adsorption at 77 K.

surface area is observed with 2.99  $m^2/g$  for the raw material (FF) and 658.4  $m^2/g$  for the 600°C-heat-treated (C-FF) material corresponding to an increase in pore volume from 0.003 to 0.342  $cm^3/g$ .

*F. carica* L. leaves were examined by scanning electron microscopy (SEM) method for their microstructure. Fig. 3 shows some SEM images of the raw material (FF) showing a fairly smooth surface, with almost no voids or cavities as expected, since it did not undergo any treatment. However, the surface of the C-FF sample shows a relatively heterogeneous surface, as well as the presence of cavities, as a result of activation. Table 3 shows the elementary analysis values of the raw *F. carica* L. leaves and the prepared activated carbon (C-FF). Based on the results, we conclude that the leaves biomass is rich in carbon (>50%) making it a good precursor for activated carbon production.

The main functional groups of *F. carica* L. leaves before and after treatment (C-FF) are shown in Fig. 4 and reported in Table 4. Noticeably, peaks are higher for the FF sample and lower for the C-FF one, due to activation. The presence of hydroxyl, carbonyl groups, and aromatic compounds is an evidence of the lignocellulosic

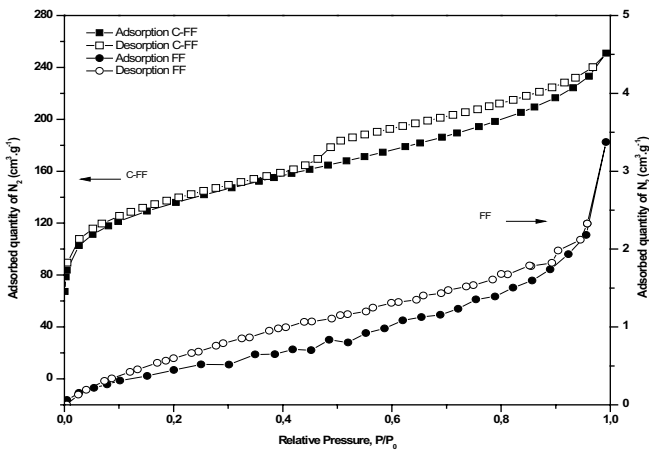


Fig. 2.  $N_2$  adsorption–desorption isotherms at 77 K onto FF and C-FF samples.

structure of *F. carica* L. leaves. The high amount of the carboxylic functional groups on the surface as obtained from Boehm's method accounts for the  $pH_{ZPC}$  (Fig. 5) value in accordance with the literature [30,32].  $H_3PO_4$  as a strong oxidant, can oxidize surface atoms to be positively charged by causing them to lose electrons. Oxygen at the same time gaining these electrons would be negatively charged and could bind to the surface oxides [32]. Most *F. carica* L. leaves bands such as the 1,430; 1,377; 1,314; 1,095; and 1,060  $cm^{-1}$  bands disappeared after heat treatment at 600°C; others have shifted slightly or decreased in intensity.

Photoelectrons binding energies of the FF and C-FF samples surface groups were studied by XPS as shown in Fig. 6 [33,34]. Results show that the peak spectra at 532 and 284 eV indicate the presence of O and C, respectively. C1s peaks can be integrated into three independent sub-bands which are assigned to carbon in the C–C (284.4 eV), C–O–C (285.3 eV), and O–C=O (288.6 eV) links.

Table 3

Elementary analysis and functional groups of FF and C-FF samples

Ultimate analysis (%)	FF sample	C-FF sample
C	53.58	88.01
O	38.25	10.36
Al	0.11	/
Si	6.37	0.12
S	0.09	0.40
Cl	/	0.34
Ca	1.60	0.32
Zn	/	0.45
Functional groups (meq/g g) from Boehm titration		
Basic	0.75	0
Carboxylic acid	0.15	1.25
Lactonic	0.08	0.75
Phénolic	0.60	0.25

The appearance of O1s peaks at 532.5 and 533.4 eV, could be due C–O and C=O bond states present in the samples [35]. According to the results of elemental analysis presented in Table 3, the surface of C-FF contains 88.01% and 10.36% of C and O elements, respectively, indicating that all functional groups are composed mainly of C, O, and optionally H which is in agreement with IRFT results.

### 3.2. Effect of Conventional parameters on adsorption

Equilibrium time, adsorbent dose, solution pH, and temperature are important parameters for the determination of optimal values. These parameters were evaluated prior to the adsorption tests.

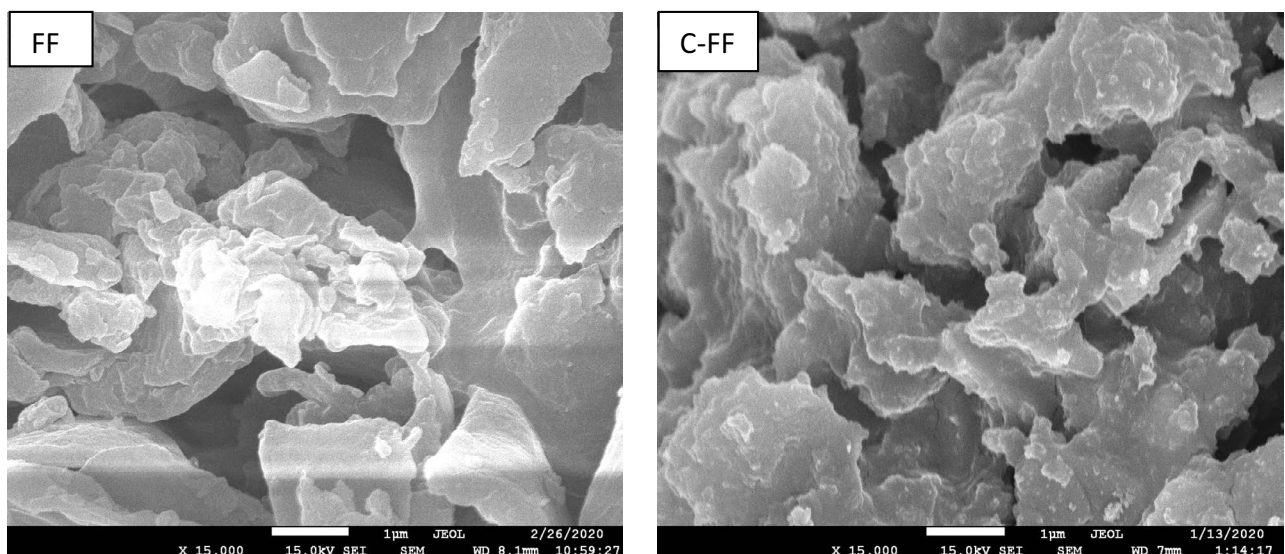


Fig. 3. SEM images of the raw *Ficus Carica* L. leaves (FF) and treated one (C-FF).

Table 4  
Characteristic wave numbers for *Ficus carica L.* leaves before and after treatment

Raw material (FF)		Treated material (C-FF)	
Band position (cm <sup>-1</sup> )	Assignment	Band position (cm <sup>-1</sup> )	Assignment
3,437–3,339	H-bonded O–H stretch, broad-strong	3,404	Stretc. Vibr. of H-bonded groups
2,949–2,869	C–H stretch for sp <sup>3</sup> carbon (weak)		N–H stretch (single medium band)
1,627	C=C stretch (medium)	2,927–2,857	sp <sup>3</sup> C–H stretch (weak)
1,430	–C–H bending variable	1,621	C=C stretch (weak)
1,377	N–O symmetric stretch	1,172–1,055	P–O stretch
1,238–1,156	C–H wag (–CH <sub>2</sub> X) weak	947	P–O–C stretch
1,095–954	C–O stretch (ether) weak		
777–653	C–Cl stretch		

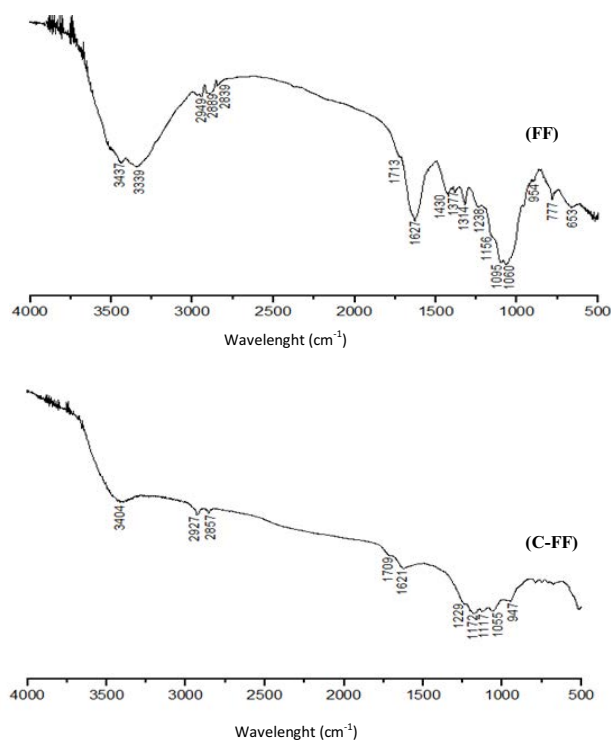


Fig. 4. FT-IR Spectra of FF and C-FF samples.

### 3.2.1. Contact time effect

Two initial concentrations of 20 and 50 mg/L at 25°C at the solution of initial pH (without adjustment) were taken as starting points for the study of the effect of contact time (ranging from 0 to 180 min) on paracetamol and amoxicillin removal onto the prepared activated carbon.

Fig. 7 shows that removal rate (%) of both substances is rapid in the initial stage due to many vacant sites but gradually stabilizes over time to equilibrium (180 min). From Fig. 7, we can see that a time of 60 min was enough to reach equilibrium. No major in the removal rate change was noticed after this time interval. The corresponding adsorption capacities of paracetamol and amoxicillin at this time were respectively 98.25% and 91.69% (for  $C_{\text{initial}} = 20$  mg/L), and 94.16% and 84.63% (for  $C_{\text{initial}} = 50$  mg/L).

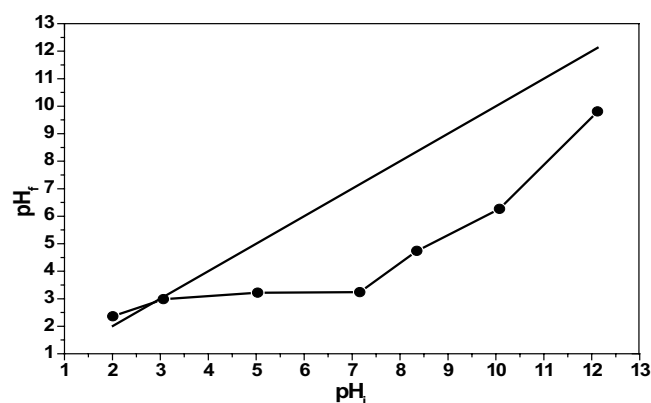


Fig. 5. pH of zero Point of charge ( $\text{pH}_{\text{zpc}}$ ) for C-FF sample.

### 3.2.2. Adsorbent mass effect

The effect of adsorbent mass on the removal of each emerging pollutant was studied in the 1–8 g/L range for an initial concentration of 50 mg/L at ambient temperature and initial solution pH. Fig. 8 shows that the adsorption rate of each emergent pollutant increases as the adsorbent mass increases. This is due to the increase of active sites and contact surface. Adsorption tends to stabilize until saturation is reached, corresponding to a maximum rate of 96.26% and 70.27% for paracetamol and amoxicillin, respectively, at an optimum activated carbon dose of 4 g/L.

### 3.2.3. pH effect

It is well-known that pH can influence not only the surface charge of most adsorbents but also the ionization degree of pharmaceuticals [36]. The percentage removal of paracetamol on C-FF as a function of pH did not change significantly. For alkaline pH values, it decreased slightly from 95.1% to 86.80%. Therefore, amount of paracetamol adsorbed in acidic media is slightly greater than those adsorbed in basic media. In this studied pH range, paracetamol ( $\text{pK}_a = 9.38$ ) is mainly in its molecular form [37]. Similar findings were reported in the literature where the adsorption on paracetamol onto cork bark, Yohimbe

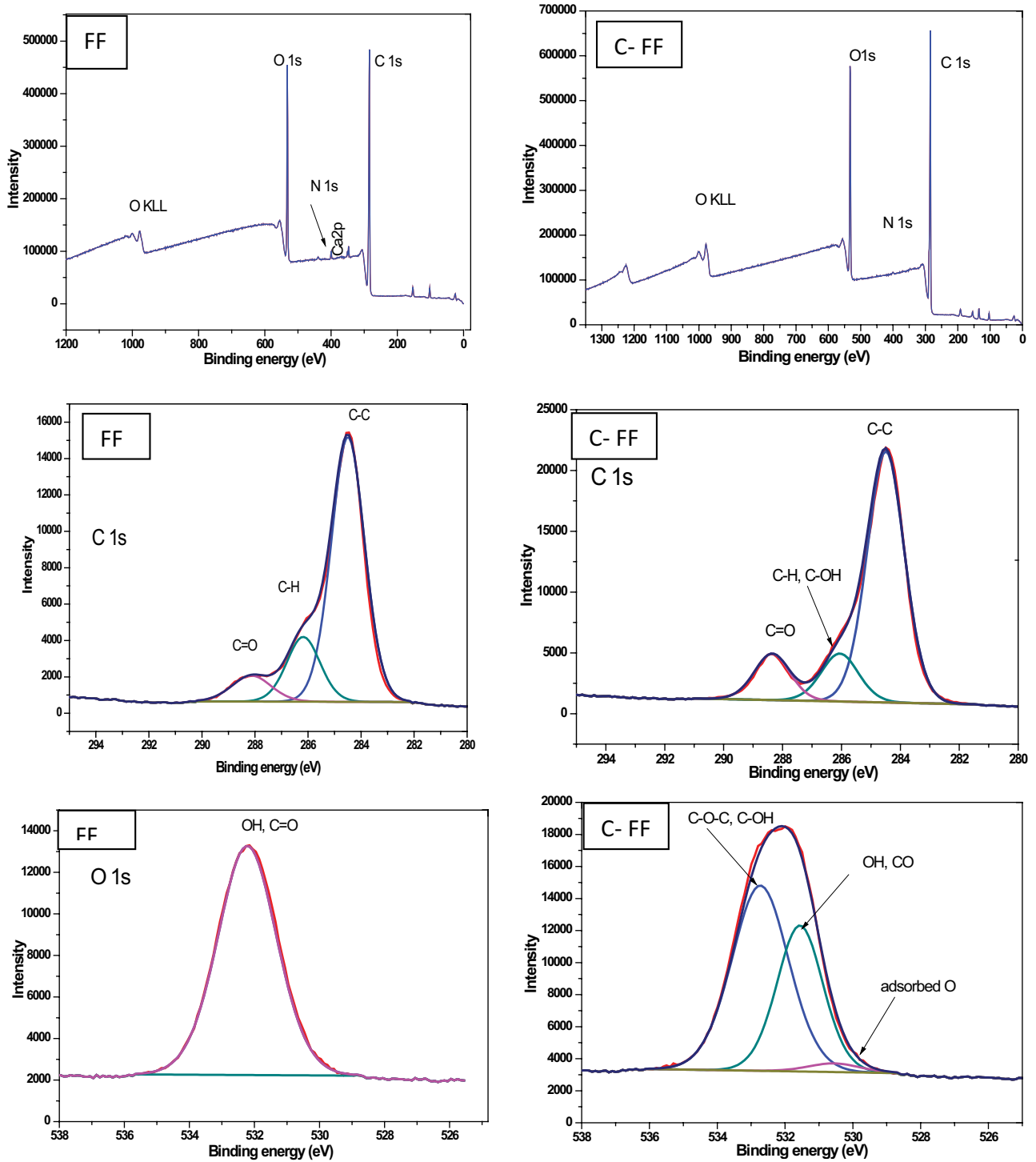


Fig. 6. Continued

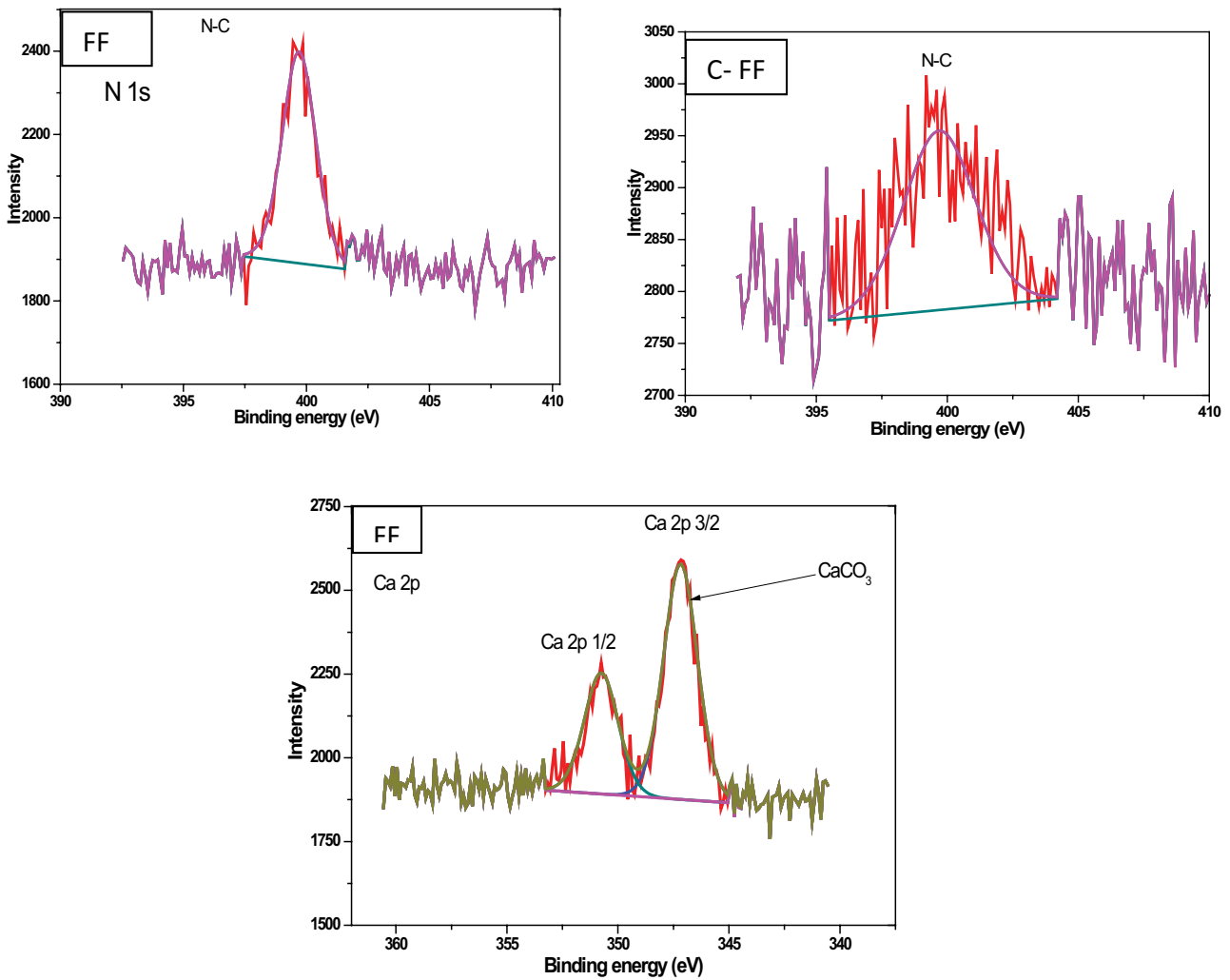


Fig. 6. XPS analyses of FF and C-FF samples.

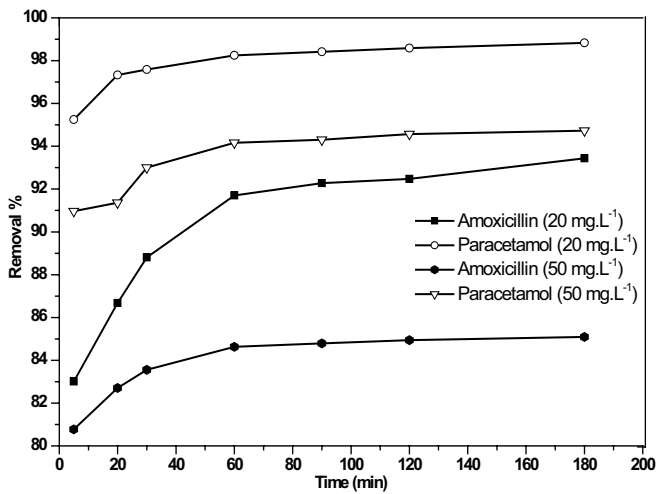


Fig. 7. Time effect on paracetamol and amoxicillin removal onto C-FF sample.

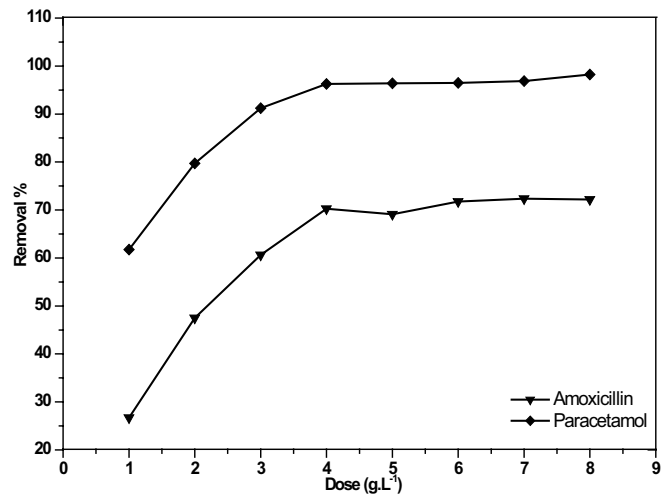


Fig. 8. Material dosage effect on paracetamol and amoxicillin removal by C-FF sample.

bark, and the grape stalk was not pH-dependent, with a slight change in adsorption capacity. It is clear that electrostatic interactions are not responsible for the adsorption of paracetamol onto C-FF. The interactions might be dispersive and possibly of hydrogen bond type [38]. Unlike for paracetamol, the solution pH has a large influence on amoxicillin adsorption as it can modify its charge. This is probably due to the nature of the amoxicillin molecule which has three pKa values of 2.4 (carboxyl), 7.4 (amine), and 9.6 (phenol) [26], so the molecule's charge is pH-dependent. As shown in Fig. 9, the highest adsorption capacity of amoxicillin onto C-FF was found to be at the initial solution pH.

For a solution of pH = 5.3, ( $pK_{a1} < pH < pK_{a2}$ ), amoxicillin is in its molecular (dominant) form and is best adsorbed in this form. The same pH greater than  $pH_{ZPC}$  indicating that the C-FF surface is negatively charged. For pH values ranging between  $pK_{a2} < pH < pK_{a3}$  and higher than  $pK_{a3}$ , amoxicillin, and the carbon surface are both negatively charged, which results in repulsive interactions between the adsorbent and the adsorbate. These results indicate that the C-FF-amoxicillin interactions are

pH-dependent, with a decrease in adsorption capacity observed at an initial pH greater than 8.

### 3.3. Modeling of adsorption isotherms

For a better description of the adsorption phenomena, we applied the non-linear forms of the three most commonly used adsorption isotherms equations, namely Langmuir, Freundlich, and Temkin models. They are summarized in Table 5.

#### 3.3.1. Langmuir isotherm [39]

It is widely used. It assumes that adsorption occurs at specific homogeneous sites within the adsorbent with no further adsorption taking place at a site once filled (Eq. (5)).

#### 3.3.2. Freundlich isotherm

This model [40] assumes that adsorption tests taking place on heterogeneous adsorbent surfaces (Eq. (6)).

#### 3.3.3. Temkin isotherm

[41] is a semi-empirical model often used in chemisorption description. It assumes that the energy of adsorption is a linear function of the surface coverage due to adsorbent–adsorbate interactions (Eq. (7)).

The values of the determination coefficient ( $R^2$ ) show that for amoxicillin, the adsorption data are well-described in the following order: Freundlich model < Temkin model < Langmuir model, but for paracetamol, the description of the data as follows: Freundlich model < Langmuir model < Temkin model. Temkin model was also representative and the positive values of  $b_T$  related to the heat of sorption for all cases studied suggest the existence of weak sorbent–sorbate interactions.

All isotherm models presented in Fig. 10, satisfactorily describe the adsorption of both emerging pollutants by the C-FF adsorbent. According to Langmuir's model, we can therefore conclude that paracetamol and amoxicillin settle on well-defined solid sites. Each site is likely to adsorb only one adsorbate molecule and the

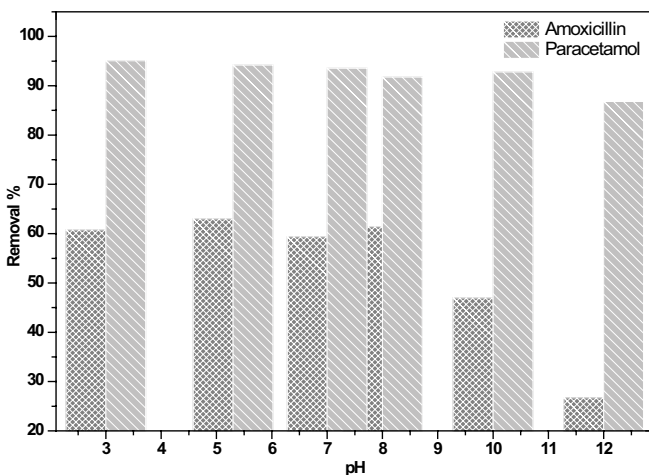


Fig. 9. Effect of pH on % removal of paracetamol and amoxicillin onto C-FF sample.

Table 5  
Non-linear forms of Langmuir, Freundlich, and Temkin isotherms

Isotherm	Nonlinear form	Parameters
Langmuir:	$q_e = \frac{bK_L C_e}{1 + K_L C_e} \quad (5)$	$q_e$ : mass adsorbed/g of adsorbent (mg/g) $C_e$ : equilibrium concentration (mg/L) $b$ : maximum adsorption capacity (mg/g) $K_L$ : constant related to net enthalpy
Freundlich:	$q_e = K_F C_e^{1/n} \quad (6)$	$K_F$ : constant related to adsorption capacity $n$ : constant related adsorption intensity $T$ : absolute temperature (K)
Temkin:	$q_e = \frac{RT}{b_T} \ln(K_T C_e) \quad (7)$	$R$ : universal gas constant (8.314 J/mol K) $b_T$ : constant related to the sorption heat (J/mol) $K_T$ : equilibrium constant corresponding to the maximum binding energy (L/mol)

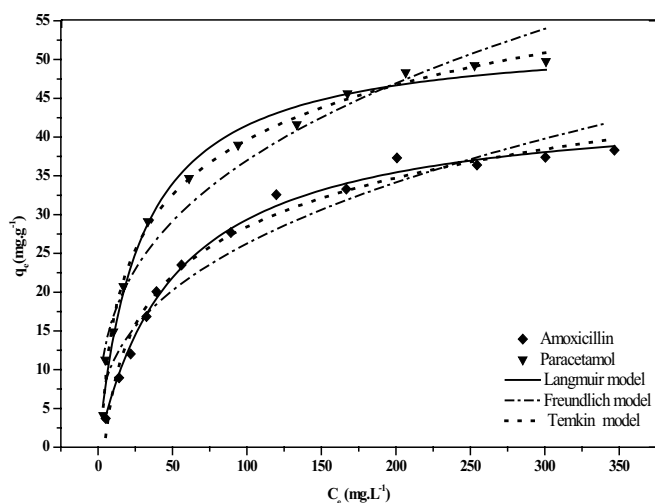


Fig. 10. Adsorption isotherms of paracetamol and amoxicillin onto C-FF sample.

adsorption energy at all sites is identical and independent of the presence of adsorbed species at other sites (surface energetically homogenous).

Isotherm parameters obtained from the curves by the different models are given in Table 6.

We can see that the maximum adsorption capacity obtained by C-FF at 600°C is 44.67 and 53.28 mg/g for amoxicillin and paracetamol, respectively compared to other adsorbents [26,42–46] reported in the literature and summarized in Table 7, implying that the *F. carica* L. leaves can be efficiently used in removing both pollutants from wastewater. Determination coefficients alone are not sufficient to determine the best isothermal model to represent the experimental data as they are generally greater than 0.90 for all three models used in this study, but the Langmuir model seems to correspond better to the experimental data with  $R^2 \geq 0.99$ , indicating that the uptake of both substances takes place as a monolayer adsorption.

### 3.4. Modeling adsorption kinetics

Kinetics study provides information not only on the adsorption mechanism but also on the transfer mode of

Table 6  
Langmuir, Freundlich, and Temkin parameters for amoxicillin and paracetamol removal onto C-FF

Models	Parameters	Amoxicillin	Paracetamol
Langmuir	$b$ (mg/g)	44.67	53.28
	$K_L$ (L/mg)	0.0192	0.0352
	$R^2$	0.994	0.987
Freundlich	$K_f$ (mg/g)	4.607	7.591
	$n$	2.650	2.910
	$R^2$	0.930	0.954
Temkin	$K_T$ (L/mg)	0.226	0.485
	$b_T$ (J/mol)	9.115	10.212
	$R^2$	0.979	0.994

adsorbates from the liquid to the solid phase. Indeed, several kinetic models have been developed to describe adsorption kinetics. The most commonly used models are:

#### 3.4.1. Lagergren's equation

The original adsorption-controlled model of Lagergren [47] is largely used for the adsorption of solute from a liquid solution. It considers adsorption to be limited by the formation of the bond between the solute and the active site and is given by the following equation:

$$\log(q_e - q_t) = \log q_{e,1} - \frac{k_1}{2.303} t \quad (8)$$

where  $q_e$  and  $q_t$  (mg/g) are the amount of pollutant adsorbed at equilibrium and at time  $t$  (min), respectively,  $k_1$  ( $\text{min}^{-1}$ ) is the pseudo-first-order adsorption rate constant,  $t$  (min) is the contact time.  $q_e$  and  $k_1$  determined from the intercept and slope of  $\log(q_e - q_t)$  vs.  $t$  plots.

#### 3.4.2. Pseudo-second-order equation

Developed by Ho and McKay [48] given by Eq. (7), is probably the most popular model used to describe adsorption kinetics, especially for new and novel sorbent materials:

Table 7  
Maximum adsorption capacities of various adsorbents for paracetamol and amoxicillin removal from aqueous solutions

Polluants	Adsorbants	$q_{\max}$ (mg/g)	Ref.
Amoxicillin	Granular activated carbon	3.16	[26]
	Bentonite	44.66	[42]
	Activated carbon from Vinewood	2.69	[43]
	Activated carbon from Olive stones	57.04	[44]
	C-FF	44.67	This work
Paracetamol	Olive stones at 700°C	37.12	[45]
	Date pits at 700°C	29.74	[45]
	Activated carbon from Spent tea leaves	59.17	[46]
	C-FF	53.28	This work

$$\frac{t}{q_i} = \frac{1}{k_2 q_e^2} + \frac{1}{q_e} t \tag{9}$$

where  $k_2$  (g/mg min) is the rate constant of the second-order equation.  $q_e$  and  $k_2$  determined from the intercept and slope  $t/q_i$  vs.  $t$  plots.

3.4.3. Intra-particle diffusion

The intra-particle diffusion model proposed by Weber–Morris [49] given by Eq. (8) was used in this study to explore the diffusion mechanism. The  $q_t$  vs.  $t^{0.5}$  plots may theoretically present one straight line in which the intraparticle diffusion is alone the rate-limiting step or multi-linearities indicating then; the overall biosorption process may be controlled either by more than one step, such as film or external diffusion, pore diffusion, surface diffusion, and adsorption on the pore surface, or a combination of at least two steps:

$$q_t = k_{int} \sqrt{t} + C \tag{10}$$

where  $k_{int}$  (mg/g min<sup>1/2</sup>) is the intra-particle diffusion rate constant, and  $C$  (mg/g) is a constant related to the thickness of the boundary layer.  $C$  is the intercept and  $k_{in}$  is the slope determined from Weber–Morris plots ( $q_t$  vs.  $t^{0.5}$ ).

The discrepancy between the experimental and the calculated equilibrium adsorption capacities ( $q_{e,exp}$  and  $q_{e,calc}$ ) and lower determination coefficients (Table 8) means kinetic data for both substances does not obey the pseudo-first model (Fig. 11). On the other hand, the pseudo-second-order model describes better the kinetic data as  $q_{e,exp} \approx q_{e,calc}$  and higher  $R^2$  values, implying that this model is more representative (Fig. 12).

The almost linear behavior of the intraparticle diffusion curve not passing through the origin, suggests that intraparticle diffusion is not the only mechanism that controls the adsorption process of the two emerging pollutants, but also that other kinetic models may control the adsorption rate as shown in Fig. 13. This also confirms that the

adsorption of paracetamol and amoxicillin is a multi-step process (two differentiated steps are detected) involving adsorption on the external surface and inward diffusion

3.5. Thermodynamic study

Thermodynamic parameters of the adsorption of paracetamol and amoxicillin onto C-FF such as the standard free energy ( $\Delta G^\circ$ ), enthalpy ( $\Delta H^\circ$ ), and entropy ( $\Delta S^\circ$ ) can be related to the distribution coefficient  $K_d$  of the dissolved substance between the solid phase and the liquid phase by following relationship equations [50]:

$$\Delta G^\circ = \Delta H^\circ - T\Delta S^\circ = -RT \ln K_d \tag{11}$$

where  $K_d$  is the distribution coefficient characterizing the affinity of the solute for the adsorbent, and can be expressed as follows:

$$K_d = \frac{q_e}{C_e} = \frac{(C_0 - C_e) \times V}{C_e \times m} \tag{12}$$

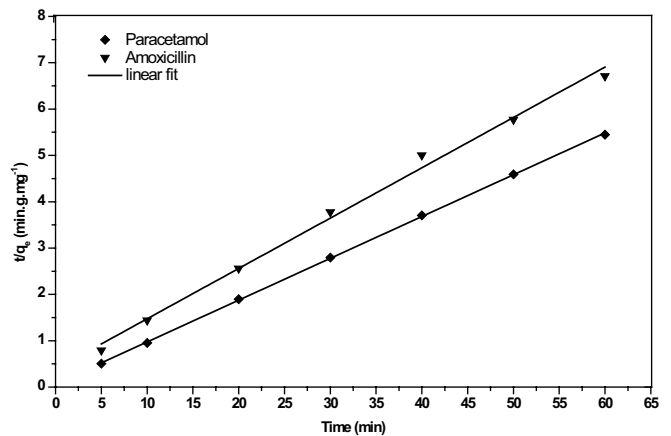


Fig. 12. Pseudo-second-order adsorption kinetics of paracetamol and amoxicillin onto C-FF.

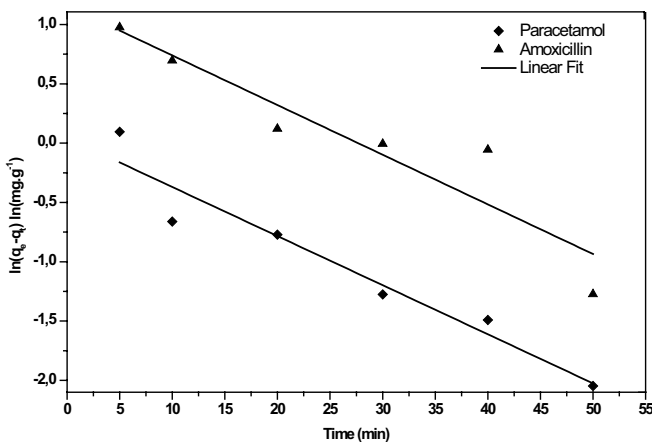


Fig. 11. Pseudo-first-order adsorption kinetics of paracetamol and amoxicillin onto C-FF.

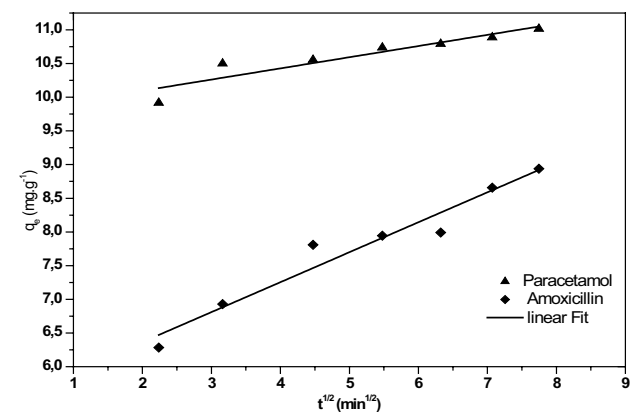


Fig. 13. Intra-particle diffusion kinetics of paracetamol and amoxicillin onto C-FF.

where  $q_e$  is the adsorption capacity (mg/g),  $C_e$  and  $C_0$  are the equilibrium and initial concentration respectively (mg/L),  $m$  is the adsorbent mass (g),  $V$  is the adsorbate volume (mL),  $T$  is the absolute temperature (K), and  $R$  is the universal gas constant (8.314 J/mol K).

Thermodynamic functions can be evaluated graphically (Fig. 14) from the intercept and slope of  $K_d$  vs.  $T^{-1}$  plots of the following equation:

$$\ln K_d = \frac{\Delta S}{R} - \frac{\Delta H}{RT} \quad (13)$$

For the adsorption process to be effective, the  $\Delta G^\circ$  must be negative ( $\Delta G^\circ < 0$ ). This is the case for both emerging pollutants by the C-FF adsorbent implying, therefore, the spontaneity of the adsorption process. In general, a value of  $\Delta G^\circ$  ranging between 0 and  $-20$  kJ/mol is compatible with the electrostatic interaction between the adsorption sites and the adsorbed species (physical adsorption).

The exothermic nature of paracetamol adsorption ( $\Delta H^\circ < 0$ ) is also accounted for by the decrease in its % removal at high temperatures as shown in Table 9. This can be explained by the weakening links between the pollutant and the active C-FF sites. In addition, solubility also increases, resulting in a stronger solute–solvent interaction than solute–adsorbent interactions, resulting in a decrease of paracetamol adsorption.

The negative value of  $\Delta S^\circ$  suggests that the sticking of paracetamol molecule on the adsorbent surface lowers randomness. As for the adsorption of amoxicillin, the

positive value of  $\Delta S^\circ$  shows an increase in disorder at the solid–liquid interface during its endothermic ( $\Delta H^\circ > 0$ ) and spontaneous ( $\Delta G^\circ < 0$ ) adsorption onto C-FF.

### 3.6. Desorption study

Desorption study of both pollutants were performed since it is a very important step in the reuse of adsorbent and pollutant recovery. It is described as the inverse of the adsorption process, through which the adsorbed molecules are detached from the substrate, allowing a generation of the porosity saturated with the pollutant. The phenomenon may help to clarify the mechanism for the removal and recovery of micropollutants and the recycling of used adsorbents, which in turn can reduce costs and protect the environment.

The monitoring of the desorption kinetics was carried out by separately contacting an exact volume of 250 mL of distilled water with 1 g of saturated activated carbon C-FF with a capacity of 30 mg/g of amoxicillin and 35 mg/g of paracetamol, in a ground-necked flask placed in a Soxhlet apparatus.

As time passes (progressively) the solvent becomes enriched with desorbed substances (their boiling temperature must be much higher than that of the extracting solvent).

The distilled water in the flask is renewed every 2 h for an overall time of 18 h, the reading of the concentration of the solution rich in emerging desorbed pollutant was determined spectrophotometrically at maximum wavelengths values mentioned in Table 1.

Table 8

Kinetic parameters of the pseudo-first-order, pseudo-second-order, and intra-particle diffusion model of paracetamol and amoxicillin adsorption onto C-FF

	Parameters	Paracetamol	Amoxicillin
Pseudo-first-order	$q_{e,exp}$ (mg/g)	11.02	8.94
	$q_{e,calc}$ (mg/g)	1.05	3.18
	$k_1$ (min <sup>-1</sup> )	0.8414	0.0419
	$R^2$	0.9225	0.8449
Pseudo-second-order	$q_{e,calc}$ (mg/g)	11.08	9.20
	$k_2$ (g/mg min)	0.1156	0.0305
	$R^2$	0.9998	0.9940
Intra-particle diffusion	$k_{int}$ (mg/g min <sup>0.5</sup> )	0.1659	0.4445
	$C$ (mg/g)	9.7645	5.4765
	$R^2$	0.8428	0.9426

Table 9

Thermodynamic parameters of paracetamol and amoxicillin adsorption onto C-FF

	$\Delta H$ (kJ/mol)	$\Delta S$ (kJ/mol K)	$-\Delta G$ (kJ/mol)			
			298 K	303 K	313 K	318 K
Paracetamol	-18.57	-36.22	7.62	7.40	7.17	7.09
		% Removal	95.37	94.73	94.03	93.60
Amoxicillin	16.61	56.54	0.59	0.94	1.21	1.44
		% Removal	83.47	85.25	86.41	87.34

As shown in Fig. 15, the amount desorbed is relatively higher at the early stage of extraction and gradually stabilizes. The molecules adsorbed on the low energy sites and on the outer surface of the activated carbon are desorbed first, however, the molecules adsorbed on the inner layers of the adsorbent can only be desorbed with the increase of the purification time which leads to bonds weakening between the adsorbate molecules and the adsorbent.

Paracetamol was difficult to desorb (25%) because of large quantities initially adsorbed on the internal wall while the desorption rate of amoxicillin is higher (91%) meaning that it is easily detached because it is mainly adsorbed on C-FF external surface due to its size.

#### 4. Conclusion

The main objective of this research work was the preparation of an activated carbon from *F. carica* L. fig leaves (C-FF) by simultaneous activation for the treatment of emerging pollutant-laden wastewater. A set of standard instrumental and wet chemical techniques was used to characterize the obtained material. Treatments were found

to enhance the specific surface area of *F. carica* L. leaves species significantly relative to their inactivated state (FF), that is, from 2.99 to 658.4 m<sup>2</sup>/g. A quick equilibrium time was reached for batch adsorption experiments at ambient temperature. Amoxicillin retention was found to be significantly influenced by pH. Kinetics study of both emerging pollutants shows that this process generally conforms to pseudo-second-order kinetics. Adsorption isotherms indicate that paracetamol is better adsorbed by C-FF than amoxicillin due to the different structure of the tested compounds. The Langmuir model was found to better describe the adsorption process of both tested emerging pollutants on the prepared activated carbon.

This study first of all, confirmed the efficacy of activated carbon prepared in the laboratory from agro waste to eliminate emergent substances from aqueous media, and opens up a number of research prospects and development of materials applicable to water pollution control, including the need to test other impregnation ratios as well as other methods of valorization of this type of waste.

#### Acknowledgments

Authors wish to thank the General Directorate of Scientific Research and Technological Development and the General Direction of Higher Education and Training (Ministry of Higher Education and Scientific Research, Algeria) for their financial support – National PRFU project (Mostaganem University) Code: B00L01UN270120180003 01/01/2018.

#### References

- [1] T. Deblonde, C. Cossu-Leguille, P. Hartemann, Emerging pollutants in wastewater: a review of the literature, *Int. J. Hyg. Environ. Health*, 214 (2011) 442–448.
- [2] J. Radjenović, M. Petrović, D. Barceló, Fate and distribution of pharmaceuticals in wastewater and sewage sludge of the conventional activated sludge (CAS) and advanced membrane bioreactor (MBR) treatment, *Water Res.*, 43 (2009) 831–841.
- [3] J. Rivera-Utrilla, M. Sánchez-Polo, M.Á. Ferro-García, G. Prados-Joya, R. Ocampo-Pérez, Pharmaceuticals as emerging contaminants and their removal from water. A review, *Chemosphere*, 93 (2013) 1268–1287.
- [4] J.-M. Pépin, Impacts Écotoxicologiques de Certains Médicaments Dans L'environnement, Université de Sherbrooke, 2006.
- [5] K. Fent, A.A. Weston, D. Caminada, Ecotoxicology of human pharmaceuticals, *Aquat. Toxicol.*, 76 (2006) 122–159.
- [6] G.W. Aherne, J. English, V. Marks, The role of immunoassay in the analysis of microcontaminants in water samples, *Ecotoxicol. Environ. Saf.*, 9 (1985) 79–83.
- [7] K. Kümmerer, Éd., *Pharmaceuticals in the Environment: Sources, Fate, Effects and Risks*, 3rd ed., Springer-Verlag, Berlin, Heidelberg, 2008.
- [8] M. Zupanc, T. Kosjek, M. Petkovšek, M. Dular, B. Kompore, B. Širok, Ž. Blažeka, E. Heath, Removal of pharmaceuticals from wastewater by biological processes, hydrodynamic cavitation and UV treatment, *Ultrason. Sonochem.*, 20 (2013) 1104–1112.
- [9] A.F. Almomani, M. Shawaqfah, R.R. Bhosale, A. Kumar, Removal of emerging pharmaceuticals from wastewater by ozone-based advanced oxidation processes, *Environ. Prog. Sustainable Energy*, 35 (2016) 982–995.
- [10] B.E. Benny Marie, B. Laura, V. Naddeo, V. Belgiorno, M. Daniel G. de Luna, C.B. Florencio Jr., Removal of pharmaceuticals from

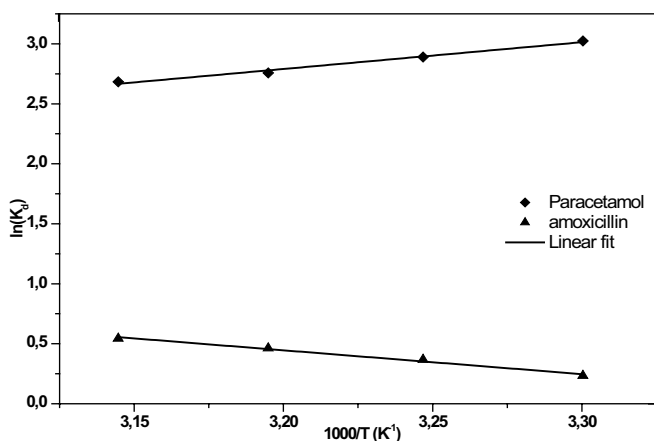


Fig. 14.  $\ln K_d$  vs.  $1/T$  plots of paracetamol and amoxicillin adsorption onto C-FF.

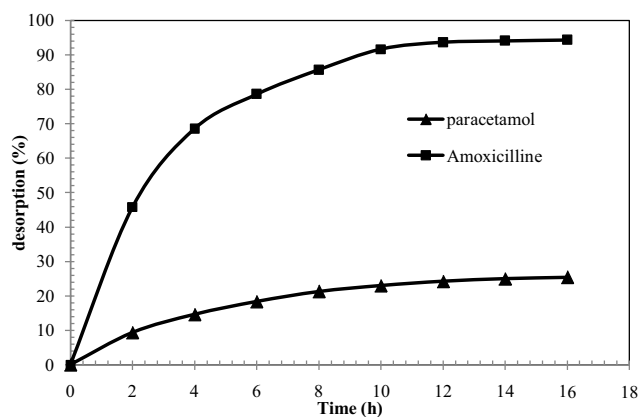


Fig. 15. Emergent pollutants desorption kinetics from C-FF sample at solution pH of 5.58.

- wastewater by intermittent electrocoagulation, *Water*, 9 (2017) 1–15, doi: 10.3390/w9020085.
- [11] B.K. Zaied, M. Rashid, M. Nasrullah, A.W. Zularisam, D. Pant, L. Singh, A comprehensive review on contaminants removal from pharmaceutical wastewater by electrocoagulation process, *Sci. Total Environ.*, 726 (2020), doi: 10.1016/j.scitotenv.2020.138095.
- [12] S. Masson, L. Reinert, S. Guittonneau, L. Duclaux, Cinétiques et isothermes d'adsorption de micropolluants sur un tissu et un feutre de carbone activé, *J. Water Sci.*, 28 (2015) 207–213.
- [13] M.D. Ruthven, Principles of Adsorption and Adsorption Processes, John Wiley & Sons, Wiley-Interscience Publication, New York, 1984.
- [14] V. Bernal, L. Giraldo, J.C. Moreno-Piraján, Physicochemical properties of activated carbon: their effect on the adsorption of pharmaceutical compounds and adsorbate-adsorbent interactions, *J. Carbon Res.*, 4 (2018) 1–20, doi: 10.3390/c4040062.
- [15] A.L. Cazetta O.P. Junior, A.M.M. Vargas, A.P. da Silva, X. Zou, T. Asefa, V.C. Almeida, Thermal regeneration study of high surface area activated carbon obtained from coconut shell: characterization and application of response surface methodology, *J. Anal. Appl. Pyrolysis*, 101 (2013) 53–60.
- [16] A. Sartape, A. Mandhare, P. Salvi, D. Pawar, P. Raut, M. Anuse, S. Kolekar, Removal of Bi(III) with adsorption technique using coconut shell activated carbon, *Chin. J. Chem Eng.*, 20 (2012) 768–775.
- [17] M. Termoul, B. Bestani, N. Benderdouche, M. Belhakem, E. Naffrechoux, Removal of phenol and 4-chlorophenol from aqueous solutions by olive stone-based activated carbon, *Adsorpt. Sci. Technol.*, 24 (2016) 375–387.
- [18] M. Benallou Benzekri, N. Benderdouche, B. Bestani, N. Douara, L. Duclaux, Valorization of olive stones into a granular activated carbon for the removal of Methylene blue in batch and fixed bed modes, *J. Mater. Environ. Sci.*, 9 (2018) 272–284.
- [19] B.S. Girgis, A.N.A. El-Hendawy, Porosity development in activated carbons obtained from date pits under chemical activation with phosphoric acid, *Microporous Mesoporous Mater.*, 52 (2002) 105–117.
- [20] A.A. Attia, B.S. Girgis, N.A. Fathy, Removal of methylene blue by carbons derived from peach stones by  $H_3PO_4$  activation: batch and column studies, *Dyes Pigm.*, 76 (2008) 282–289.
- [21] N. Douara, B. Bestani, N. Benderdouche, L. Duclaux, Sawdust-based activated carbon ability in the removal of phenol-based organics from aqueous media, *Desal. Water Treat.*, 57 (2016) 5529–5545.
- [22] Y. Guo, D.A. Rockstraw, Physicochemical properties of carbons prepared from pecan shell by phosphoric acid activation, *Bioresour. Technol.*, 98 (2007) 1513–1521.
- [23] M. Al Bahri, L. Calvo, M.A. Gilarranz, J.J. Rodriguez, Activated carbon from grape seeds upon chemical activation with phosphoric acid: application to the adsorption of diuron from water, *Chem. Eng. J.*, 203 (2012) 348–356.
- [24] B.V. Pereira, G.N. Matus, M.J. Costa, A.C.A. Dos Santos, E.C. Silva-Zacarin, J.B. do Carmo, B. Nunes, Assessment of biochemical alterations in the neotropical fish species *Phalloceros harpagos* after acute and chronic exposure to the drugs paracetamol and propranolol, *Environ. Sci. Pollut. Res.*, 25 (2018) 14899–14910.
- [25] A. Macías-García, J. García-Sanz-Calcedo, J.P. Carrasco-Amador, R. Segura-Cruz, Adsorption of paracetamol in hospital wastewater through activated carbon filters, *Sustainability*, 11 (2019) 1–11.
- [26] M.A.E. de Franco, C.B. de Carvalho, M.M. Bonetto, R.d.P. Soares, L.A. Féris, Removal of amoxicillin from water by adsorption onto activated carbon in batch process and fixed bed column: kinetics, isotherms, experimental design and breakthrough curves modelling, *J. Cleaner Prod.*, 161 (2017) 947–956.
- [27] ASTM, Standard Test Method for Determination of Iodine Number of Activated Carbon, ASTM Annual Book, Section 15, Active Standard D4607–94, 1999.
- [28] B. Bestani, N. Benderdouche, B. Benstaali, M. Belhakem, A. Addou, Methylene blue and iodine adsorption onto an activated desert plant, *Bioresour. Technol.*, 99 (2008) 8441–8444.
- [29] C. Kaewpravit, E. Hequet, N. Abidi, J.P. Gourlo, Application of methylene blue adsorption to cotton fiber specific surface area measurement: part I. Methodology, *J. Cotton Sci.*, 2 (1998) 164–173.
- [30] H.P. Boehm, Surface oxides on carbon and their analysis: a critical assessment, *Carbon*, 40 (2002) 145–149.
- [31] S. Attouti, B. Bestani, N. Benderdouche, Chemical surface modification of seaweed species for cationic dyes removal from simulated water, *Indian J. Environ. Prot.*, 40 (2020) 462–472.
- [32] L.A. Al-Khateeb, S. Almotiry, M.A. Salam, Adsorption of pharmaceutical pollutants onto graphene nanoplatelets, *Chem. Eng. J.*, 248 (2014) 191–199.
- [33] A.P. Terzyk, The influence of activated carbon surface chemical composition on the adsorption of acetaminophen (paracetamol) *in vitro*: part II. TG, FTIR, and XPS analysis of carbons and the temperature dependence of adsorption kinetics at the neutral pH, *Colloid Surf., A*, 177 (2001) 23–45.
- [34] X. Ma, H. Yang, L. Yu, Y. Chen, Y. Li, Preparation, surface and pore structure of high surface area activated carbon fibers from bamboo by steam activation, *Materials*, 7 (2014) 4431–4441.
- [35] N. Zhuo, Y. Lan, W. Yang, Z. Yang, X. Li, X. Zhou, Y. Liu, J. Shen, X. Zhang Adsorption of three selected pharmaceuticals and personal care products (PPCPs) onto MIL-101(Cr)/natural polymer composite beads, *Sep. Purif. Technol.*, 177 (2017) 272–280.
- [36] R.C. Ferreira, O.M. Couto Jr., K.Q. Carvalho, P.A. Arroyo, M.A.S.D. Barros, Effect of solution pH on the removal of paracetamol by activated carbon of dende coconut mesocarp, *Chem. Biochem. Eng. Q.*, 29 (2015) 47–53.
- [37] I. Villaescusa, N. Fiol, J. Poch, A. Bianchi, C. Bazzicalupi, Mechanism of paracetamol removal by vegetable wastes: the contribution of  $\pi$ - $\pi$  interactions, hydrogen bonding and hydrophobic effect, *Desalination*, 270 (2011) 135–142.
- [38] G.N. Rolinson, A.M. Geddes, The 50th anniversary of the discovery of 6-aminopenicillanic acid (6-APA), *Int. J. Antimicrob. Agents*, 29 (2007) 3–8.
- [39] I. Langmuir, The constitution and fundamental properties of solids and liquids, *J. Am. Chem. Soc.*, 38 (1916) 2221–2295.
- [40] H.M.F. Freundlich, Over the adsorption in solution, *J. Phys. Chem.*, 57 (1906) 385–470.
- [41] M.I. Temkin, V. Pyzhev, Kinetics of ammonia synthesis on promoted iron catalysts, *Acta Physicochim. URS*, 12 (1940) 217–222.
- [42] S. Budyanto, S. Soedjono, W. Irawaty, N. Indraswati, Studies of adsorption equilibria and kinetics of amoxicillin from simulated wastewater using activated carbon and natural bentonite, *J. Environ. Prot. Sci.*, 2 (2008) 72–80.
- [43] G. Moussavi, A. Alahabadi, K. Yaghmaeian, M. Eskandari, Preparation, characterization and adsorption potential of the  $NH_4Cl$ -induced activated carbon for the removal of amoxicillin antibiotic from water, *Chem. Eng. J.*, 217 (2016) 119–128.
- [44] L. Limousy, I. Ghouma, A. Ouederni, M. Jeguirim, Amoxicillin removal from aqueous solution using activated carbon prepared by chemical activation of olive stone, *Environ. Sci. Pollut. Res.*, 24 (2017) 9993–10004.
- [45] F. Medjdoub, K. Louhab, A. Hamouche, Comparative study of the adsorption of paracetamol from aqueous solution on olive stones and date pits, *Desal. Water Treat.*, 104 (2018) 225–233.
- [46] S. Wong, Y. Lim, N. Ngadi, R. Mat, O. Hassan, I.M. Inuwa, B. Nurul, H.L. Jiun, Removal of acetaminophen by activated carbon synthesized from spent tea leaves: equilibrium, kinetics and thermodynamics studies, *Powder Technol.*, 338 (2018) 878–886.
- [47] S. Lagergren, Zur theorie der sogenannten adsorption gelöster stoffe, *Kungl. Svens. Vetenskapsakad. Handl.*, 24 (1898) 1–39.
- [48] Y.S. Ho, G. McKay, Kinetic models for the sorption of dye from aqueous solution by wood, *Process Saf. Environ.*, 76 (1998) 183–191.
- [49] W.J. Weber, J.C. Morris, Kinetics of adsorption on carbon from solution, *J. Sanitary Eng. Div.*, 89 (1963) 31–60.
- [50] D. Hu, L. Wang, Adsorption of amoxicillin onto quaternized cellulose from flax oil: kinetic, equilibrium and thermodynamic study, *J. Taiwan Inst. Chem. Eng.*, 64 (2016) 227–234.